This is a postprint version of the following published document:

A. Bautista (et al.). *Corrugated stainless steels embedded in mortar for 9 years: corrosion results of non-carbonated, chloride-contaminated samples*.
Construction and Building Materials 93 (2015) pp. 350–359
DOI: 10.1016/j.conbuildmat.2015.04.060

Corrugated stainless steels embedded in mortar for 9 years: Corrosion results of non-carbonated, chloride-contaminated samples

A. Bautista, E.C. Paredes, F. Velasco *, S.M. Alvarez

Materials Science and Engineering Department – IAAB, Universidad Carlos III de Madrid, Avda. Universidad nº 30, 28911 Leganés, Madrid, Spain

HIGHLIGHTS

- 5 corrugated stainless steel grades are studied in chloride contaminated mortars.
- E_{corr} and EIS are used for monitoring, and polarizations tests are also carried out.
- Spontaneous corrosion only appears in low Ni austenitic S20430 at partial immersion.
- S32205 duplex does not show any sign of corrosion even at anodic high polarizations.

ABSTRACT

Mortar samples reinforced with 5 different corrugated stainless steels were tested for 9 years in 2 different conditions: partial immersion (PI) in 3.5% NaCl, and chloride addition to the mortar and exposure to high relative humidity (HRH). The monitoring during the exposures was carried out with corrosion potential (E_{corr}) and electrochemical impedance spectroscopy (EIS) measurements. A year before finishing (after 8 years of exposure), the reinforced mortar samples were anodically polarised to obtain more information about the pitting resistance of the passive layers formed under the different conditions. The last year of exposure was established to study the progress or repassivation of the pits. The PI is the most aggressive testing condition and it causes low intensity corrosion in S20430 austenitic stainless steel after 7 years of exposure. The S32205 duplex stainless steel shows very good corrosion behaviour.

Keywords:
Stainless steel
Steel reinforced mortar
EIS
Polarisation
Passivity
Pitting corrosion

1. Introduction

The high alkalinity of concrete creates an environment that protects steel against corrosion. However, the life expectancy of concrete structures is affected by corrosion of steel reinforcements, because of an aggressive attack of chloride ions or as a result of carbonation [1,2]. The presence of chloride in the environment increases the risk of pitting corrosion in these steels. When chloride levels are extremely high, the passive layer of the steel can be destroyed in large areas of the reinforcement and general corrosion takes place [3].

Stainless steels are more corrosion resistant to chloride than traditional carbon steel reinforcements [4]. The study of the corrosion behaviour of stainless steel reinforcements, to replace carbon steel reinforcements in highly aggressive environments, has been a subject of research in recent years [5,6]. The performance of stainless steel reinforcements in structures under dynamic loads has started to be studied in depth [7], but the majority of the research up to now is focused on the corrosion behaviour of the material. Most studies of the corrosion behaviour of stainless steel are based on the use of solutions simulating those found in concrete pores. Almost all authors agree that the high alkalinity of simulated pore solutions improves the corrosion behaviour of stainless steel in chloride contaminated environments [8–13].

Most published studies deal with the influence of alloying elements in simulated solutions. Traditionally, the UNS S30400 and S31600 austenitic stainless steel grades have been analysed [9,12,14,15]. Some researchers detect no difference between the pitting corrosion resistance of both materials in solution tests [10,16]. However, others conclude that there is a slightly better behaviour of S31600 grade [17,18].

The low alloyed, austenitic UNS S20430 stainless steel has been proposed as an economic alternative to traditional stainless steels for use in reinforced concrete structures, due to its corrosion performance [19]. Results in simulated pore solutions have shown

* Corresponding author. Tel.: +34 91 624 9485; fax: +34 91 624 9430.
E-mail address: fvelasco@ing.uc3m.es (F. Velasco).

slightly less pitting corrosion resistance than UNS 30400 steel [20,21]. The analysis of the passive layer in alkaline environments has revealed that its composition is slightly less protective than that of traditional austenitic steels [17]. UNS S20430 could be about 35 40% cheaper than traditional austenitic S30400 grade, though the difference depends on the strong volatility of nickel price in the market.

Duplex stainless steels have appeared in the market as a note worthy option for concrete structures [11,22 24]. The preliminary studies in simulated solutions suggest a very good corrosion beha viour of UNS S32205 duplex grade [8,17]. This grade could result only about 5 10% more expensive than S30400, but about 30% cheaper than S31600.

The stainless steels used as reinforcing bars in concrete have suffered a heavy rolling process that strongly modifies the microstructural characteristics of their surface [13,25]. The impor tance of the forming process in the corrosion behaviour of corru gated stainless steel bars has been recently studied [13,22].

There are scarce studies on the corrosion behaviour of corru gated stainless steels embedded in concrete or mortar, especially when compared to the large number of studies published using simulated pore solutions. There are a few old studies performed on mortar and concrete, but focused on less interesting steel grades than those used today, or on steels not processed as corrugated reinforcements [26,27]. More recent studies only cover a limited time period (1.5 3 years) [6,23,28 30].

Nevertheless, concrete and mortar studies are very important for confirming the durability of corrugated stainless steels, because there are four key aspects in the early stages and in the develop ment of the corrosion process that simulated pore solutions are not able to reproduce:

(a) The crevices present in the rebar/mortar interface, which can play an important role in the corrosion mechanism [31].
(b) The presence of a dense, lime rich layer of hydration prod ucts in the steel concrete interface [32], which can hinder the attack.
(c) The difficulty for oxygen diffusion is different in mortar than in solution and it often limits the corrosion rate [33]. The oxygen concentration at the reinforcement surface is a key factor that usually restricts or inhibits the attack in immersed structures. However, in aerial structures exposed to environments with moderate relative humidity (when the concrete pores are not saturated), the oxygen diffusion to the reinforcement is easier than in solution.
(d) The resistivity of the concrete, that depends on the porosity and the water saturation level of the pores, can be much higher than the resistivity of the testing solutions. There is a correlation between concrete resistivity, the corrosion ini tiation period and the corrosion propagation [1,34]. In aerial structures, the concrete resistivity can often control the cor rosion rate when the environment is dry. When there is humidity in the air, concrete is able to absorb it, facilitating the corrosion attack. It this case, oxygen gains access to the reinforcement, since the diffusion distance through the aqueous layer is small and the environment resistivity is low [35].

The main objective of this study is to analyse the corrosion behaviour of different corrugated stainless steel grades embedded in mortar, which have been exposed to highly aggressive environ ments. The electrochemical behaviour has been monitored for 9 years, using non destructive techniques such as electrochemical impedance spectroscopy (EIS) and corrosion potential measure ments (E_{corr}). In addition, a year before the end of the exposure per iod, anodic polarisation tests were performed to determine the probability of pitting corrosion in the steels that were still in a pas sive state. The samples were left an additional year in order to analyse the evolution of the attack provoked with these polarisa tion tests. In the present paper, results obtained in non carbonated mortar samples are shown and discussed.

2. Experimental

Five different corrugated stainless steel bars were considered in the study. The chemical composition of the stainless steels, their diameter and their tensile strength are shown in Table 1. Traditional carbon steel corrugated bars (Table 2) were also included for reference.

The corrugated bars were partly embedded in mortar with a cement/sand/water ratio of 1/3/0.6 (w/w). CEM II/B-L 32.5N was the cement type used to prepare the mortar. The sand was standardized CEN-NORMSAND (according to DIN EN 196-1 standard). The water/cement ratio was high, as it is quite usual in experimental tests [6,36,37]. Bearing in mind that a good quality concrete can have a water/cement ratio of about 0.4, the use of this mortar samples will imply that the capillarity porosity volume fraction will be about 2 times higher after the curing period than that of good quality material [38], and nearly 3 times higher after the complete hydration of the cement [38]. However, this type of samples allows to obtain results in a reasonable period of time and can reproduce one of the conditions the stainless steel reinforcements are specially advised: light, porous concrete coatings.

Half of the mortar samples were manufactured with 3% $CaCl_2$, weighed in relation to the amount of cement (equivalent to 1.9% of Cl by wt. of cement). This chloride was selected as calcium oxide is the main compound of cement, and this way no new cations were added. Its concentration is slightly higher than those sometimes used to test the behaviour of carbon steel [39] or galvanised steel [36] in mortar, and it is inside the range of that used to test some stainless steels [29].

Cylindrical mortar samples were used to minimize heterogeneities in the electrical signal distribution during the EIS monitoring (Fig. 1a). The thickness of the mortar cover was always 1.5 cm, independently of the diameter of the bar (Table 1). The length from the end of the corrugated bar to the bottom of the mortar sample was also 1.5 cm. The surface of the bars exposed to the mortar-air interface was isolated to avoid interference in the study (mainly carbonation) as other authors have previously done [29]. The exposed length of the bar in mortar was always 3 cm. All cross-sections of the bars embedded in mortar were previously polished to 320# and passivated with HNO_3 (50% by wt. of acid, 50 s) in the laboratory, reproducing the process carried out on the corrugated surfaces of the bars in industry. Moreover, the cross section of the bars are much less prone to corrosion than strained surface [40], thus assuring that all electrochemical information is related to processes taking place on the surface of the bars. This procedure minimizes the risk of crevice that shielding the cross-sections with resin could seldom cause.

After their manufacture, the reinforced mortar samples were cured for 30 days at approximately 92–93% relative humidity (RH). After this time, for mortars as these – without any special addition or supplementary cementitious material – it could be assumed that about the 75% of the hydration reactions of the cement have already taken place [38]. Then, they began their exposure period under two different conditions. The samples manufactured with chlorides were exposed to 92–93% RH (condition labelled as HRH). The samples without chlorides were partially immersed (PI) in 3.5% (w/w) NaCl solution (equivalent to 2.64% of Cl by wt.) and at 92–93% RH. In this case, the level of the solution was maintained at the same height as the middle of the length of the bars exposed in the mortar. Curing processes and exposures were always carried out at room temperature, and two samples were manufactured for each material and exposure condition.

The electrochemical monitoring of the corrosion behaviour during the 8-year exposure period was carried out using E_{corr} and EIS measurements. To obtain the E_{corr} values, a saturated calomel electrode (SCE) was used. For the EIS measurements, a three-electrode configuration was used. The surface of corrugated bar exposed to the mortar acted as working electrode. The reference electrode was a SCE placed on the upper part of the sample (Fig. 1b). The counter-electrode was a copper cylinder, with a diameter slightly larger than that of the mortar sample. To assure good contact between the mortar and the counter-electrode, and the mortar and the SCE, wet pads were used. The EIS spectra were acquired using a perturbation signal of 10 mV (rms) of amplitude, from 10^2 to 10^{-3} Hz. 5 points/decade were measured.

After the 8-year exposure period, the reinforced mortar samples were submitted to anodic polarisation tests. The tests started from the E_{corr} and were based on short potentiostatic steps. Each step increased the potential in 20 mV. The length of the steps close to E_{corr} was of 10 min. When the potential of 100 mV vs SCE was surpassed, the length of the steps increased to 1 h. Fig. 2a shows an example of the signal applied and of the obtained current response. The increase of the length of the steps is due to greater difficulties of stabilization of the current signal at increasing anodic overpotentials; Fig. 2b shows a detail of signals, where the shape of the current transients caused by the increasing potential steps is shown. The polarisation steps finished at 900 mV vs. SCE.

Table 1
Chemical composition (w/w), diameter and tensile strength of the studied stainless steels.

Stainless steel			Diameter (mm)	Main alloying elements (%)											Tensile strength (MPa)
UNS	AISI	EN		S	C	Ti	Si	Mn	Cr	Ni	Mo	N	Cu	Fe	
S20430	204Cu	1.4597	5	0.002	0.049	0.003	0.23	8.26	16.12	1.89	0.015	0.130	2.65	Bal.	918
S30400	304	1.4301	8	0.002	0.063	0.004	0.31	1.42	18.33	8.12	0.297	0.050	0.32	Bal.	1035
S31603	316L	1.4404	10	0.006	0.021	0.003	0.21	1.67	17.05	10.25	2.171	0.47	0.32	Bal.	805
S31635	316Ti	1.4571	12	0.001	0.029	0.251	0.45	1.21	16.68	11.25	2.232	0.020	0.41	Bal.	860
S32205	2205	1.4462	12	0.001	0.029	0.027	0.39	1.72	22.49	4.72	3.221	0.174	0.24	Bal.	1156

Table 2
Chemical composition (w/w) and diameter of the studied carbon steel.

Diameter (mm)	C	S	P	Si	Mn	Cr	Ni	Mo	Cu	Fe
10	0.245	0.002	0.030	0.55	0.76	0.24	0.093	0.02	0.60	Bal.

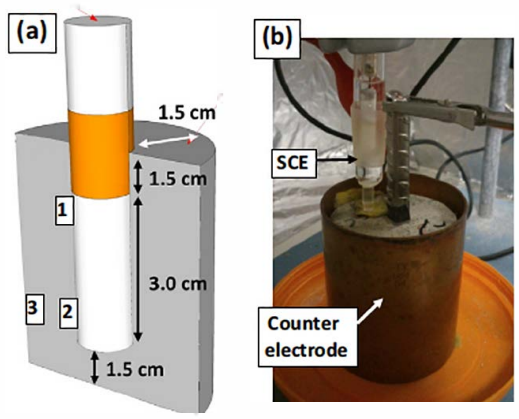

Fig. 1. Reinforced mortar specimens manufactured for the study: (a) scheme of the samples showing the regions where the chloride content was measured (as 1–3); (b) image of the samples during the electrochemical measurements.

The current value plotted on the polarisation curves used in this study corresponds to the stabilization value of the current after each potential step. The analysis procedure of the transients was based on the potential-step method, where the contribution of the ohmic drop through the mortar can easily be distinguished from the electrochemical response of the reinforcements [41]. The length chosen for the potential steps allows us to obtain more reliable results than the traditional polarisation curves carried out at a much higher sweeping rate, as the stabilization of the current after the pulses is slower as polarizations increases. Moreover, the use of steps allow achieving potentials as high as water decomposition, not able to reach with polarisation resistance.

After the polarisation tests, the samples remained for 1 year in PI or HRH to allow progress or possible repassivation of the provoked pits. As only anodic polarisation was carried out, without backwards sweep of current, the growth of pits could be limited during the test. Then, the samples were broken. The mortar cover was carefully removed and the morphology and localization of the attack on the surface of the stainless steel reinforcements were studied by scanning electron microscopy (SEM). The last year of exposure allows a more reliable evaluation by microscopy techniques of the pits.

Moreover, the total chloride content of the mortar after the 9-year exposure was measured in 3 different regions of the samples. The localization of the studied regions is marked in Fig. 1a. The quantification of the total chloride content was carried out by X-ray fluorescence (XRF) spectrometry [42]. The obtained value is the average of at least 5 measurements in each region of the samples.

3. Results and discussion

In Fig. 3, it can be seen that the chloride concentration (in relation to the mortar weight) for samples where the depassivating ion has been added during the mortar manufacturing (HRH) remains constant in all the studied regions of the mortar (Fig. 1a). This chloride level (in relation to the mortar weight) can be comparable, for example, to those found (in relation to the concrete weight) at 7 8 cm from the surface of non submerged region of a structure exposed for 60 years in a tropical marine environment [43]. Moreover, extrapolating the results obtained by other authors [44], this chloride concentration could imply about a 3% of chloride ion in the pore solution of a structure manufactured without addi tions. Though the minimum chloride concentration to provoke the corrosion of the reinforcements in concrete is a controversial issue and can be influenced by factors, this chloride level is enough to hinder passivation of carbon steel and cause its active corrosion [45].

The concentration of ions in the PI exposed samples reaches also similar values in the 3 regions after 9 years of exposure (Fig. 3), although chlorides penetrate from the outer solution by the lower half of the sample. The diffusion that has taken place

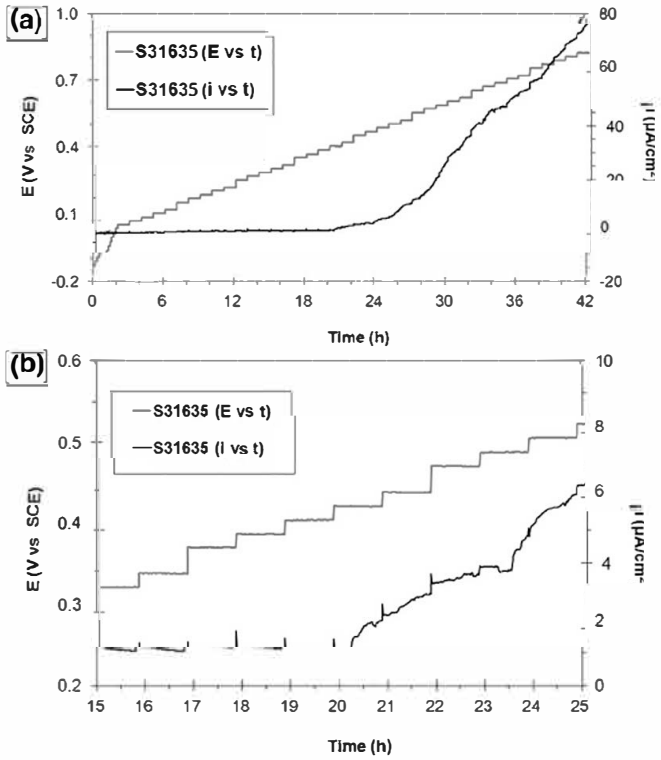

Fig. 2. Example of the potential steps applied to the mortar samples at the end of the exposure and the obtained current response: (a) test carried out for a sample reinforced with S31635 after PI; (b) detail of the data shown in (a).

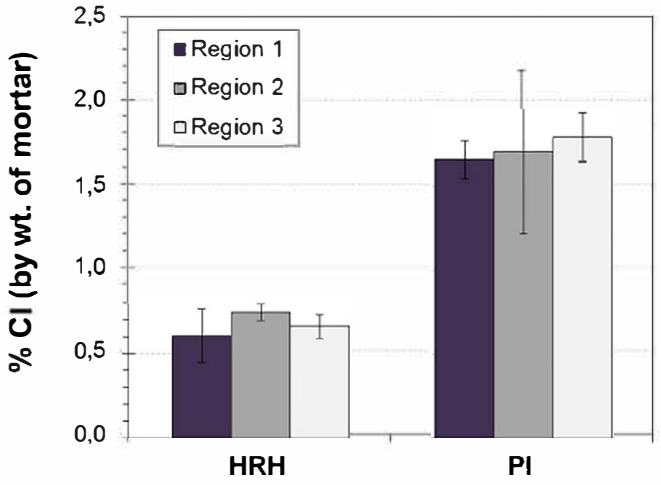

Fig. 3. Chloride concentration (% by wt. to mortar) after 9 years exposure.

during the long exposure has eliminated the possibility of formation of chloride concentration cells between the submerged and non submerged region of the PI samples. The final chloride level is about three times higher than that of HRH condition.

The E_{corr} values monitored for the corrugated bars in mortar are shown in Figs. 4 and 5. The ASTM C876 standard suggests a criterion for determining the probability of corrosion for non coated carbon steel reinforcements that has been included in the figures. Factors than can sometimes limit the reliability of the information from E_{corr} about the corrosion performance [46] can be ruled out in this case, due to the characteristics of the experimental design.

The E_{corr} evolution of the corrugated bars embedded in mortar with chloride additions and exposed to HRH can be seen in Fig. 4. After only 3 months under HRH conditions, carbon steel shows quite low E_{corr} values. A review paper has stated that these values (<−426 mV vs. SCE) are typical of a severe corrosion attack [47], and in our laboratory it has been checked that these samples were completely cracked after 6–8 months of testing. The amount of added chlorides in this mortar (Fig. 3) is high enough to provoke very aggressive corrosive attack in the carbon steel bars, as the added chloride amount surpasses the threshold values proposed for this material [45].

In HRH (Fig. 4), all the stainless steels exhibit E_{corr} values typical of the passive state during the first period of 8 years. The added chlorides, able to provoke corrosion on carbon steel bars, do not seem to affect, for the tested conditions, the performance of stainless steel bars. This confirms that stainless steel reinforcements have much higher chloride threshold values than carbon steel ones under these conditions.

Under PI conditions (Fig. 5), carbon steel bars also corrode since the first months of the exposure. This can be easily understood bearing in mind the high water/cement ratio that allows a fast diffusion of the chlorides from the solution to the bar surface through the mortar cover, that should have reach values high enough to provoke corrosion.

On the other hand, the E_{corr} of the stainless steel bars under PI (Fig. 5) tends to remain in the region where the risk of corrosion is lower than 10%, with some random values in the region with an uncertain risk of corrosion. Though this relationship between E_{corr} and corrosion probability has not been specifically validated for stainless steels, these results suggest a good corrosion performance for all the tested stainless steels but S20430 (especially bearing in mind that the resistivity of the mortar cannot mask the attack because of its wetness). After 7 years, the E_{corr} of this material exhibits values corresponding to a high risk of corrosion.

The differences found for the E_{corr} values of S20430 at the end of the exposure for both studied conditions and the trend shown for other stainless to exhibit some random values in the region of uncertainty during PI are coherent with the fact that the PI in chloride media is an especially aggressive condition. The existence of an aerated region close to a submerged region (where the oxygen access is more hindered) favours the formation of an active corrosion cell (between submerged and non submerged areas) and fosters the attack. Moreover, after a time, the chloride concentration close to reinforcements is higher for the samples exposed in PI than for the samples in HRH (Fig. 3).

With the aim of obtaining more complete information about the corrosion performance of the samples during the exposure, they have been monitored by EIS. Representative examples of the shape of the spectra corresponding to reinforcing stainless steels can be seen in Fig. 6a and b. An adequate quality of the fitting is achieved using a two time constant cascade model, as it can also be checked in the figure. Previous EIS studies in simulated pore solutions have demonstrated that the spectrum of passive stainless steels is formed by two, very overlapped, time constants [12,17,24]. During the analysis of the spectra the resistive behaviour obtained at high frequencies in the EIS spectra corresponds to the mortar resistance (R_m). The first time constant at intermediate frequencies

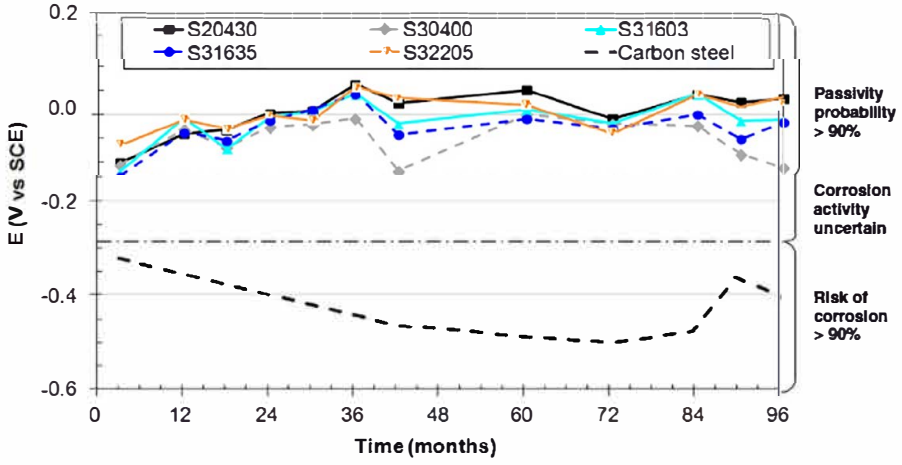

Fig. 4. E_{corr} evolution of the samples exposed to HRH (mortar with chloride additions and exposed to high RH). The evaluation of the corrosion risk following the standardized criteria for carbon steels has been included.

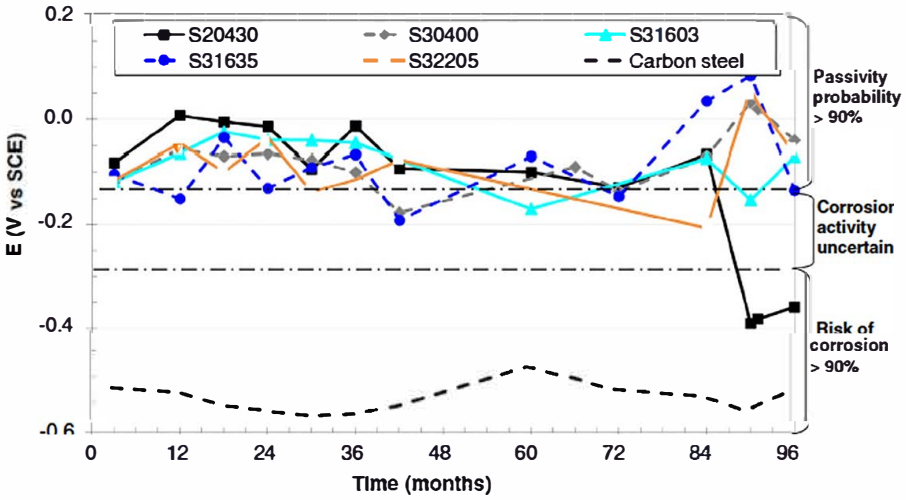

Fig. 5. E_{corr} evolution of the PI mortar samples during the 8-year exposure. The evaluation of the corrosion risk following the standardized criteria for carbon steels has been included.

has been simulated with a resistance R_{pl} and a constant phase element CPE_{pl}. This time constant has been identified with electrochemical characteristics of the passive layer, as other EIS studies of corrugated stainless steel in alkaline solutions [17] and in mortar [6] have previously done. The low frequency time constant is often identified with the corrosion process. In this case, R_t would be the charge transfer resistance of the electrochemical reaction and CPE_{dl} would simulate the capacitive behaviour of the double layer.

The proposed equivalent circuit (Fig. 6c) is typical of defective passive layers. It could be considered reasonable bearing in mind the non homogeneity that the passive layer should exhibit when it is formed on the surfaces of the corrugated stainless steel bars. Those surfaces exhibit different stress levels, and, particularly, highly stressed areas [40], thus limiting the protective ability of the passive oxides [13]. Other research groups have also chosen this equivalent circuit to simulate the electrochemical behaviour of active and passive stainless steel in solution and in mortar [6,48,49]. The work carried out in this study confirms that this model is useful to simulate the electrochemical behaviour of passive stainless steel corrugated bars embedded in mortar (Fig. 6a). Furthermore, the equivalent circuit is still valid when the E_{corr} of the stainless steel reinforcements decreases to the region of high corrosion risk, as during the last period of PI of S20430 (Fig. 6b). If only one constant is considered for the active behaviour, the error of the fitting dramatically increases; the weighed sum of squares, proportional to the average percentage error between original and calculated points, changes from 0.04 (two time constants) to 0.27 (for one time constant).

R_m is an important parameter that can control the corrosion rate, as mortar or concrete are electrolytes with moderate conductivity. In Fig. 7, the R_m values obtained from the simulation of the EIS data can be seen. For PI samples, R_m increases at the beginning of the exposure due to chemical processes that implies the curing of the cement [50] and that it is not completely hydrated after the curing period [38]. So, the mortar increases its density, and its electrical resistance. These processes determine the increases of R_m values during the first two years (Fig. 7a). Then, as the PI exposure extends, the migration of chloride ions inside the mortar from the solution prevails, and the R_m decreases. Other authors have observed somewhat similar trends for PI samples in a low quality mortar; in reference [6], R_m increases due to mortar curing during the first 3 months and then decreases due to chloride penetration. This effect is clearly visible from the third year of exposure. A certain stabilization of R_m can be guessed during the last year of exposure. This could be explained considering the fact that the chloride concentration inside the pore solution is high and the diffusion process from the external solution is hindered or slowed down.

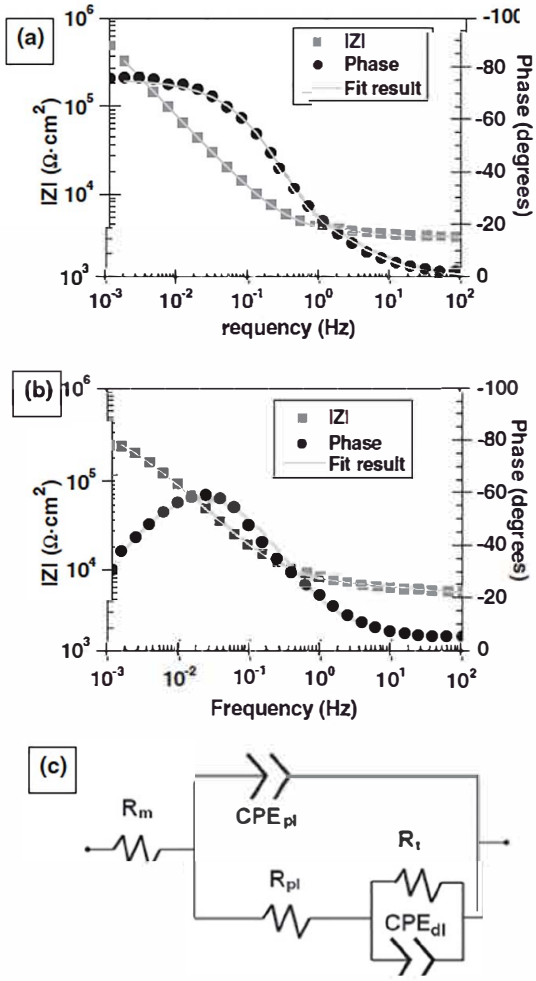

Fig. 6. Example of the experimental EIS spectra and fitting results corresponding to stainless steel reinforcements: (a) system whose E_{corr} is in the passive region (S32205 after 3 months in PI); (b) system whose E_{corr} is in the active region (S20430 after 8 years in PI); (c) equivalent circuit used to fit the experimental results.

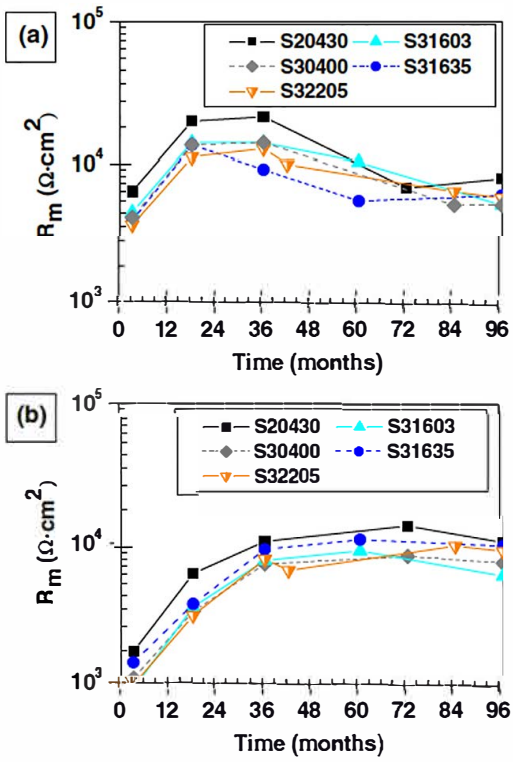

Fig. 7. Time evolution of R_m: (a) PI; (b) HRH.

When the mortar samples are manufactured with chlorides (HRH), R_m tends to increase during the first 3 years, due to the same reasons than PI samples, and later, its value remains stable (Fig. 7b), as no entry of new chlorides takes place during the exposure.

The R_{pl} values that have been obtained from the simulation of the EIS spectra can be seen in Fig. 8. In the solution tests, during the first hours, an increase in R_{pl} value has been reported due to the changes in the oxidation state on the oxides in the passive layer

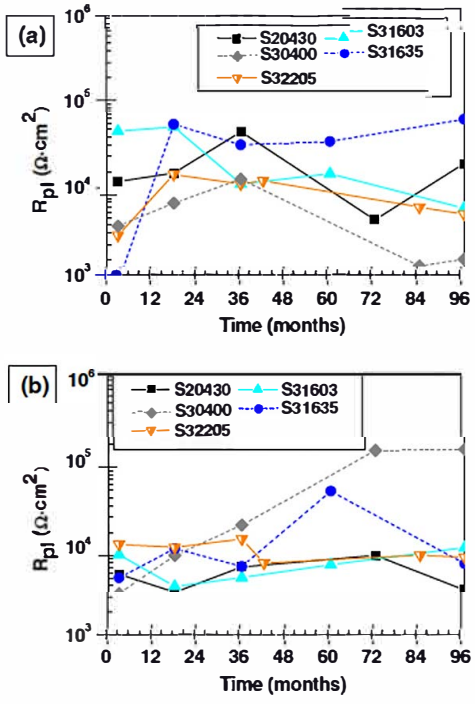

Fig. 8. Time evolution of R_{pl}: (a) PI; (b) HRH.

due to the exposure to the alkaline medium [17]. For the same type of reinforcements embedded in mortar, this trend can hardly be guessed (Fig. 8). The oscillation in R_{pl} values can probably be related to the uncertainty that implies obtaining data from spectra with such overlapped constants. Hence, it can be assumed that, after a certain time, the chemical composition and structure of the passive film reach an equilibrium with the medium, with this process taking less than 3 months. The R_{pl} values measured in mortar during the long term exposure are about 1 order of magnitude higher than those measured in solution after 1 day, so the transformation of the passive layer in the previous solutions tests was incomplete.

The non ideal capacitive behaviour that a CPE simulates is given by two numerical parameters [24]: the capacitance values, C, and the coefficient that quantifies the deviations from the ideal behaviour, n, being $CPE = 1/[C(jw)^n]$. For the CPE_{pl}, the C_{pl} and n_{pl} obtained values can be seen in Fig. 9. They are similar to those previously measured in solution for these bars [17]. In certain cases, a slight trend of n_{pl} to decrease its value with time could be guessed. This would correspond to an increase in the dispersion with frequency of the capacitive behaviour of CPE_{pl} that could reflect an increase of inhomogeneities in the passive layer with time. The testing conditions in mortar do not seem to introduce any relevant influence in the R_{pl} and C_{pl} values, though the more frequent dispersion in the values in Figs. 8a and 9a can be related to the higher aggressivity of the PI exposure.

The R_t values obtained from the EIS measurements are shown in Fig. 10. R_t values tend to increase during the first period of exposure. This trend has already been detected in short term solution tests [17,18], but it should be borne in mind that, during 18 h solution tests, R_t does not reach 10^7 Ω cm^2. After years in mortar, R_t can be as high as 10^9 Ω cm^2. That is to say, there is an improvement of the passive behaviour of the stainless steels during the first year of exposure to aggressive environments. This process seems to be faster during the PI test than during the HRH test, perhaps because of the low chloride concentration close to the reinforcements during the first months of exposure in the PI.

On the other hand, at the end of the PI exposure, a decrease of R_t values can be observed for some stainless steel grades (Fig. 10a). Low nickel austenitic stainless steel grade S20430, with E_{corr} values in the high corrosion risk zone (Fig. 5), exhibits a meaningful decrease of R_t. This information seems to confirm the corrosion attack on this grade under these conditions. On the other hand, S31635 also shows a meaningful decrease of its R_t value (Fig. 10a), when its E_{corr} is only in the upper area of the uncertain corrosion region. It is difficult to obtain reliable conclusions about these results, but certain dissolution of TiN precipitates (abundant in this material) can explain the phenomenon. It has been previously demonstrated that preferential TiN dissolution occurs at high potentials in simulated pore solutions [20]. The decrease on R_t could be the consequence of a lower corrosion resistance of the surface of the reinforcement due to the surface irregularities (cavities) caused by the dissolution of the precipitates.

As has been reported for the same reinforcements in solution tests [17] and for different passive stainless steel bars in mortar [6], the R_t values (Fig. 10) are significantly higher than R_{pl} (Fig. 8). That is to say, the charge transfer is the rate limiting step for passive reinforcements. This fact allows us to identify R_t also with the polarisation resistance in the Stern Geary equation [51] and calculate corrosion intensities, i_{corr}. Though a B about 52 mV has been traditionally proposed for passive steel in concrete [52], recent studies have calculated a higher value, about 75 mV, for this parameter [53]. Assuming $B = 75$ mV (which is the most conservative hypothesis), the i_{corr} from studied stainless steels with E_{corr} in the passive region and region with uncertain risk of corrosion (Figs. 4 and 5) would range from about 7 to nearly 0.07 nA/cm^2.

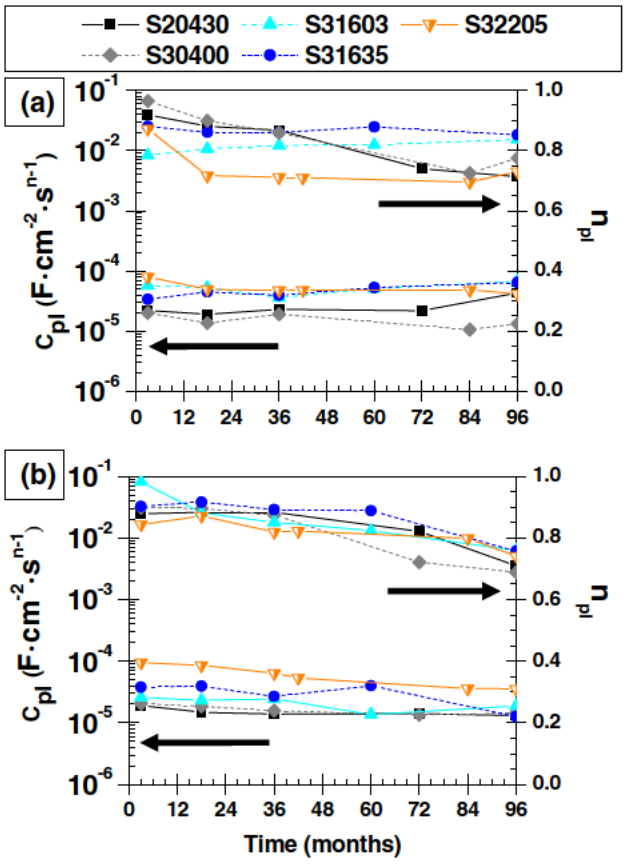

Fig. 9. Time evolution of the C_{pl} and n_{pl} parameters that define CPE_{pl}: (a) PI; (b) HRH.

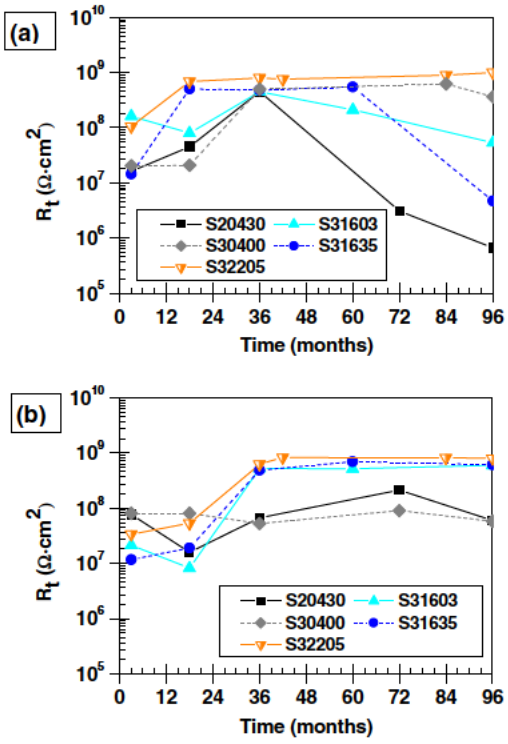

Fig. 10. Time evolution of R_t: (a) PI; (b) HRH.

Those i_{corr} are quite similar or lower than others determined for passive S30400 in concrete specimens using polarisation resistance

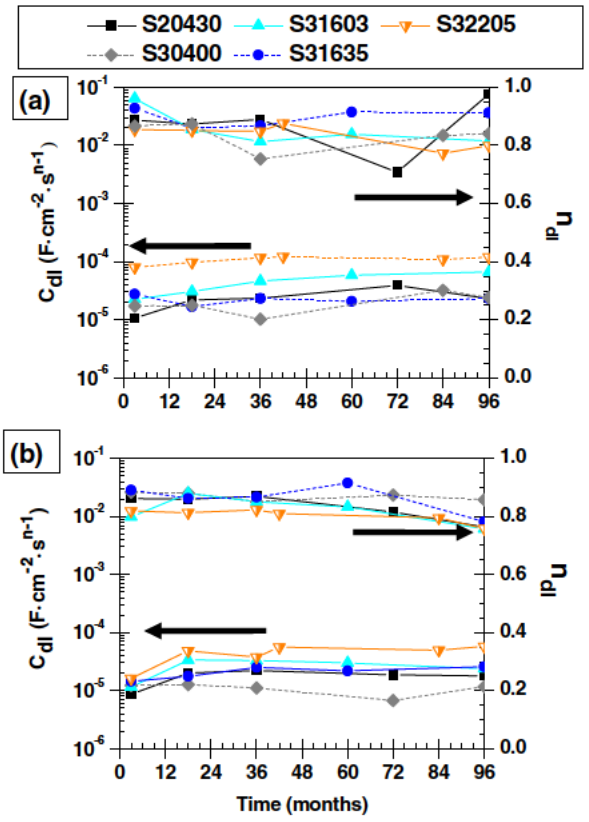

Fig. 11. Time evolution of the C_{dl} and n_{dl} parameters that define CPE_{dl}: (a) PI; (b) HRH.

measurements (about 0.01 0.1 μA/cm^2) [23,29]. The uncertainty in the determination of the corrosion rate of passive systems is unavoidable, but it is obvious that the measured i_{corr} values are able to comply with any durability requirement of reinforced structures.

Corrugated S20430 stainless steel in PI mortar exhibits E_{corr} typical of active corrosion at the end of the exposure (Fig. 5). For active steel in concrete, values of B for 15 26 mV have been reported in the literature [52,53]. Assuming again the most conservative hypothesis, with $B = 26$ mV, the i_{corr} of the S20430 steel would always be below 0.04 μA/cm^2. This corrosion rate is obviously very low and it hardly represents a meaningful risk for the durability of the structure [31]. For comparison, studies of carbon steel reinforcements in similar conditions carried out in our laboratory give corrosion rates that can oscillate approximately between 0.3 and more than 3 μA/cm^2, that to say 1 or 2 order of magnitude higher. Moreover, for carbon steel in chloride contaminated concrete slabs, i_{corr} between 0.3 and 1 μA/cm^2 have been measured [29]. Hence, the S20430 probably suffers a corrosion attack of very low intensity during the last year of the PI test.

The values obtained from the simulation of the EIS spectra for the CPE_{dl} are plotted in Fig. 11. It can be checked that the values are typical of the double layer capacitance of active and passive stainless steel reinforcements in mortar [24, 54], confirming the hypothesis that the low frequency time constant corresponds to the charge transfer process. No meaningful change is detected with time during the exposures, not even for S20430 or S31635.

After 8 years of exposure, the stainless steel reinforced samples were submitted to anodic polarisation tests. The objective was to obtain information about the quality of the passive layer under these conditions and to know how the pitting resistance of the stainless steel has been modified. Data similar to the typical polarisation curves can be obtained (Figure 12). The anodic polarizations

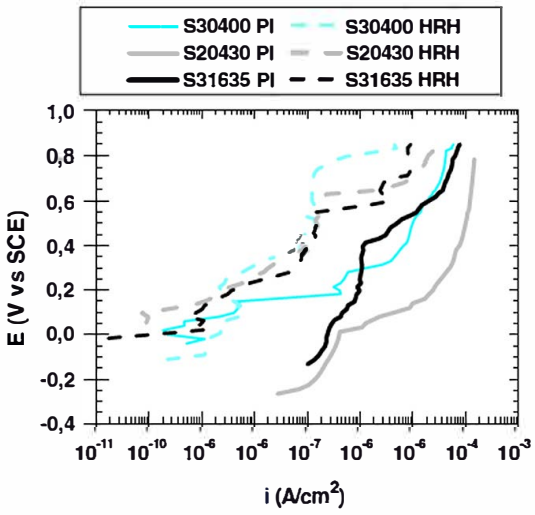

Fig. 12. Example of the results of the potential step tests when they are plotted as standard polarisation curves in an Evans diagram.

needed to reach a current density of $2{\cdot}10^{-6}$ A/cm^2 are plotted in Fig. 13 to compare different mortar samples. As has been previously mentioned, this value is typical of the corrosion rate for carbon steel reinforcements under the exposure conditions considered in the study. Moreover, it is also a value inside the range of the usual current densities used to define the pitting potential or to compare the corrosion behaviour of stainless steel reinforcements [11,20,29].

In spite of small differences detected by EIS for most of the stainless steels in both testing conditions (Figs. 8–11), after polarisation tests, it is clear that PI samples are much more prone to develop pitting corrosion than the HRH samples (Fig. 13). The length of the passive region of samples exposed to HRH seems to be able to guarantee the durability of reinforced structures in chloride contaminated environments, even when low cost, low alloyed grades as S20430 are considered. The good results for this material previously obtained in simulated pore solutions with chlorides are confirmed [20]. The potentials plotted in Fig. 13 for S30400, S31603 and S32205 in HRH seem to correspond to the oxygen evolution reaction, not to pitting corrosion. This hypothesis is based on two facts: (a) the high value of the potential where the current increase takes place (at the limit of the region of the thermodynamic stability of water); and (b) the similar potential value determined for the three materials with such different alloying elements (Table 1).

The behaviour exhibited by the S31635 (Fig. 13) can be noteworthy, as can be considered comparable with that of the less

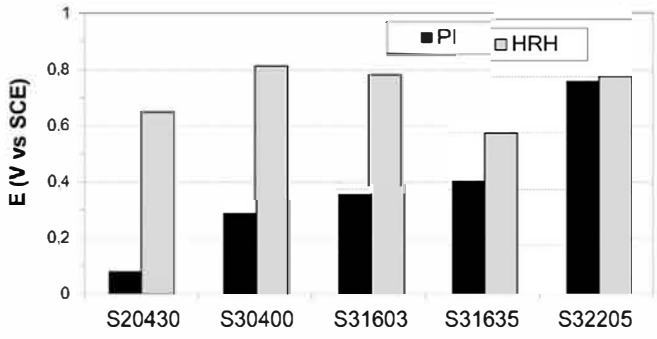

Fig. 13. Potentials needed for the reinforced samples after the 8-year exposure to reach anodic current values of $2{\cdot}10^{-6}$ A/cm^2.

alloyed, much cheaper S20430 grade. In this case, the length of the passive region is limited by the presence of TiN precipitates, being also coherent with the EIS results (Fig. 10a).

On the other hand, in the polarisation tests, all the austenitic corrugated stainless steel bars have proved to be quite sensitive to the aggressive conditions (high chloride concentration, aeration cells) created by the PI (Fig. 13). After the PI exposure, the polarisation test can cause pitting in all the grades except S32205. For this grade, potential corresponds to oxygen evolution. The very good behaviour of duplex S32205 suggested in solution tests [13,20] is again confirmed. Such a high corrosion resistance can be understood bearing in mind the highly protective nature of the passive layer formed on this grade in alkaline media, as has been proved by XPS studies [17]. The differences found in the pitting resistance between S30400 and S31603 can hardly justify the economic differences existing between both materials (the presence of Mo in S31603 makes it rather more expensive than the S30400). For highly aggressive conditions, the S32205 is a much more interesting option than S31603, somewhat cheaper and much more corrosion resistant (Fig. 13). These results should be kept in mind when a stainless steel grade is selected for structures exposed to extremely aggressive conditions and long service life is expected.

The use of S20430 in aggressive environments can be risky in the long term and it pits in PI under absence of external polarisation (Fig. 5). Though the R_t measured at E_{corr} are quite high (Fig. 10a), the current density can become dangerous in the presence of small anodic polarizations (Fig. 13). The possible limitations for the use of S20430 are coherent with the results of shorter test experiments carried out by other authors, also using PI mortar samples [6].

Life expectancy of stainless steel reinforcements in structures is difficult to evaluate, as chloride ingress into concrete is a complex process. Moreover, it is strongly affected by the characteristics of the basic components, the huge diversity of additives and the specific manufacturing procedure of the concrete. Results in this research can not be easily extrapolated to real conditions in terms of quantifiable durability. Tested mortar is porous due to high water/cement ratio, and corrosion takes place after three months in carbon steel, an unreal circumstance. Anyway, the good behaviour of the stainless steel bars in such a corrosive exposure condition is a guarantee of meaningful increase of the durability of the bars in practice, that it is more realistic than previous published solution results. These results confirm the advantages of using stainless steel bars for structures located in aggressive environments and their ability to dramatically extend the life expectancy of the structures. Obviously the specific characteristics of the passivity achieved by the stainless steels reinforcements would be conditioned by the specific features of the concrete structure and the environment.

After polarizations, the tested samples remained in PI or HRHto allow pit development or repassivation. Then, the mortar samples were broken to allow the observation of the reinforcements. No pits were observed in S32205 samples in both exposure conditions, neither in S30400 and S31603 after HRH exposure, which is coherent with the hypothesis that in these systems the current increase in polarisation tests is due to oxygen evolution. In addition, the corrosive attack in S31635 (where the polarisation had caused corrosion, as suggests results in Fig. 13) cannot be confirmed after SEM observations. These data suggest a certain ability of the S31635 grade to repassivate or highly limit the attack rate when it is exposed to mortars with a chloride contaminations, such as those of the samples tested at HRH.

Visible localised attack is clearly observed in the other stainless steel tested reinforcements. In the samples where the corrosion starts before the polarisation tests (S20430 in PI), the direct

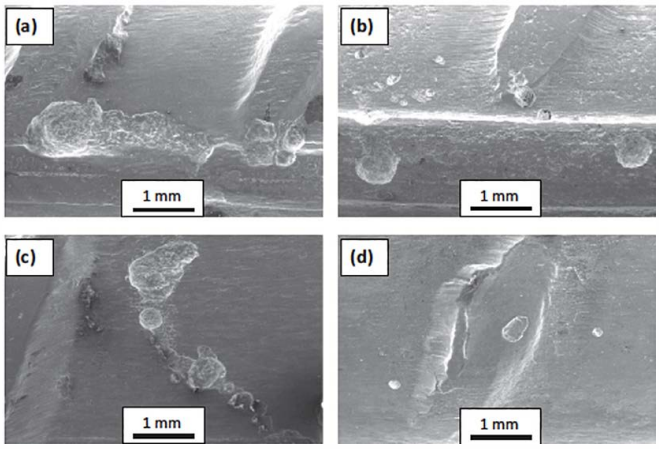

Fig. 14. Surface images of the morphology of corrosive attack caused by the anodic polarisation in the embedded reinforcements. (a) S20430 after PI; (b) S30400 after PI; (c) S31603 after PI; (d) S20430 after HRH.

observation of the attack in the surface shows very numerous, large and irregular pits (Fig. 14a).

On S30400 exposed at PI, numerous rounded pits can be observed, most of them with a location clearly related with the most strained regions of the surface of the bar (Fig. 14b). The influence of the forming process in the corrosion behaviour of stainless steels has been demonstrated in simulated pore solutions tests [13]. The cold working of the reinforcements cause microstructural changes that can affect the corrosion behaviour of the stainless steels [55] and these changes are much more pronounced in the corrugations than in other regions of the surface [40].

In S31603 and S31635 bars exposed to PI, the attack morphology is different, as can be seen in the example in Fig. 14c. The pits are irregular and quite shallow, and their location does not seem to be related to the corrugations or other more strained areas on the surface of the bars. This corrosion morphology seems less dangerous than that observed for non Mo austenitic reinforcements. However, the difference could not be due to chemical composition of the stainless steels. The lower strain level of these bars in comparison with the tested S30400 can easily explain this fact (the lower tensile strengths of the S31603 and S31635 bars in Table 1 correspond to a less heavy forming process). A heavy forming process would cause high densities of defects and dislocations in the corrugations, so these regions of the bars would become much more prone to corrosion [40].

After the HRH exposure, the only bar with visible signs of attack is the S20430. Anyway, the intensity of the attack is low in this environment, compared to that observed in other grades after PI and polarisation. A few isolated, rounded pits have been detected (Fig. 14d) after provoking the attack by anodic polarizations. Pits tend to be larger in most strained regions, but SEM observations proved that a few small pits also appear in the non corrugated region of the surface. This trend can be related to the strain level in the bar, which is between that of the S30400 and those of the S31603 and S31635 bars (Table 1).

4. Conclusions

The results presented in this study allow us to draw the following conclusions:

1. E_{corr} and EIS results show that traditional austenitic and duplex corrugated stainless steels are a very interesting option to assure the durability of reinforced structures in chloride contaminated media.
2. The partial immersion exposure in 3.5% NaCl causes a very low intensity corrosive attack in S20430 samples after 7 years of exposure.
3. The S32205 does not show corrosion in highly chloride contaminated mortar, even under partial immersion conditions and high polarizations, confirming that it is the best option for structures exposed to highly aggressive conditions.
4. No difference between the corrosion behaviour of S31603 and S30400 has been found under the studied exposure conditions.

Acknowledgements

The present work was funded by the Spanish Ministry of Science and Innovation through the Project reference BIA2007 66491 C02 02. The authors acknowledge the help of Eng. Rubén Martin with EIS spectra.

References

[1] Ann KY, Ahn JH, Ryou JS. The importance of chloride content at the concrete surface in assessing the time to corrosion of steel in concrete structures. Constr Build Mater 2009;23:239–45.
[2] Elfergani HA, Pullin R, Holford KM. Damage assessment of corrosion in prestressed concrete by acoustic emission. Constr Build Mater 2013;40:925–33.
[3] Hornbostel K, Larsen CK, Geiker MR. Relationship between concrete resistivity and corrosion rate – a literature review. Cem Concrete Comp 2013;39:60–72.
[4] Andión LG, Garcés P, Cases F, Andreu CG, Vázquez JL. Metallic corrosion of steels embedded in calcium aluminated mortars. Cem Concrete Res 2001;31:1263–9.
[5] Pérez-Quiroz JT, Terán J, Herrera MJ, Martinez M, Genesca J. Assessment of stainless steel reinforcement for concrete structures rehabilitation. J Constr Steel Res 2008;64:1317–24.
[6] Serdar M, Valek-Žulj L, Bjegović D. Long-term corrosion behavior of stainless reinforcing steel in mortar exposed to chloride environment. Corros Sci 2013;69:149–57.
[7] Cadoni E, Fenu L, Forni D. Strain rate behaviour in tension of austenitic stainless steel used for reinforcing bars. Constr Build Mater 2012;35:399–407.
[8] Moser RD, Singh PM, Kahn LF, Kurtis KE. Chloride-induced corrosion resistance of high-strength stainless steels in simulated alkaline and carbonated concrete pore solutions. Corros Sci 2012;57:241–53.
[9] Freire L, Carmezim MJ, Ferreira MGS, Montemor MF. The passive behavior of AISI 316 in alkaline media and the effect of pH: a combined electrochemical and analytical study. Electrochim Acta 2010;55:6174–81.
[10] Kouřil M, Novák P, Bojko M. Threshold chloride concentration for stainless steels activation in concrete pore solutions. Cem Concrete Res 2010;40:431–6.
[11] Alvarez SM, Bautista A, Velasco F. Corrosion behaviour of corrugated lean duplex stainless steels in simulated concrete pore solutions. Corros Sci 2011;53:1748–55.
[12] Bautista A, Blanco G, Velasco F, Martinez MA. Corrosion performance of welded stainless steels reinforcements in simulated pore solutions. Constr Build Mater 2007;21:1267–76.
[13] Paredes EC, Bautista A, Alvarez SM, Velasco F. Influence of the forming process of corrugated stainless steels on their corrosion behaviour in simulated pore solutions. Corros Sci 2012;58:52–61.
[14] Freire L, Carmezim MJ, Ferreira MGS, Montemor MF. The electrochemical behavior of stainless stel AISI 304 in alkaline solutions with different pH in the presence of chlorides. Electrochim Acta 2011;56:5280–9.
[15] Hurley MF, Scully JR. Threshold chloride concentrations of selected corrosion-resistant rebar materials compared to carbon steel. Corrosion 2006;62:892–904.
[16] Freire L, Catarino MA, Godinho MI, Ferreira MJ, Ferreira MGS, Simões AMP, et al. Electrochemical and analytical investigation of passive films formed on stainless steels in alkaline media. Cem Concrete Comp 2012;34:1075–81.
[17] Bautista A, Blanco G, Velasco F, Gutiérrez A, Soriano L, Palomares FJ, et al. Changes in the passive layer of corrugated, low Ni, austenitic stainless steel due to the exposure to simulated pore solutions. Corros Sci 2009;51:785–92.
[18] Bautista A, Blanco G, Takenouti H. EIS study of passivation of austenitic and duplex stainless steel reinforcements in simulated pore solutions. Cem Concrete Comp 2006;28:212–9.
[19] Fajardo S, Bastidas DM, Criado M, Romero M, Bastidas JM. Corrosion behaviour of a new low-nickel stainless steel in saturated calcium hydroxide solution. Constr Build Mater 2011;25:4190–6.
[20] Bautista A, Blanco G, Velasco F. Corrosion behaviour of low-nickel austenitic stainless steels reinforcements: a comparative study in simulated pore solutions. Cem Concrete Res 2006;36:1922–30.
[21] Freire L, Novoa XR, Pena G, Vivier V. On the corrosion mechanism of AISI 204Cu stainless steel in chlorinated alkaline media. Corros Sci 2008;50:3205–12.

[22] Alvarez SM, Bautista A, Velasco F. Influence of process parameters on the corrosion resistance of corrugated austenitic and duplex stainless steel. Mater Technol 2013;47:317–21.
[23] Bertolini L, Gastaldi M. Corrosion resistance of low-nickel duplex stainless steel rebars. Mater Corros 2011;62:120–9.
[24] Luo H, Dong CF, Li XG, Xiao K. The electrochemical behaviour of 2205 duplex stainless steel in alkaline solutions with different pH in the presence of chloride. Electrochim Acta 2012;64:211–20.
[25] Bautista A, Alvarez SM, Velasco F. Selective corrosion of duplex stainless steel bars in acid. Part 1: effect of the composition, microstructure and anodic polarization. Mater Corros 2015;66:347–56.
[26] Flint GN, Cox RN. The resistance of stainless steel partly embedded in concrete to corrosion by seawater. Mag Concrete Res 1988;40:13–9.
[27] Callaghan BG. The performance of a 12% chromium steel in concrete in severe marina environments. Corros Sci 1993;35:1535–41.
[28] García-Alonso MC, Escudero ML, Miranda JM, Vega MI, Capilla F, Correia MJ, et al. Corrosion behaviour of new stainless steels reinforcing bars embedded in concrete. Cem Concrete Res 2007;37:1463–71.
[29] García-Alonso MC, González JA, Miranda J, Escudero ML, Correia MJ, Salta M, et al. Corrosion behaviour of innovative stainless steels in mortar. Cem Concrete Res 2007;37:1562–9.
[30] Duarte RG, Castela AS, Neves R, Freire L, Montemor MF. Corrosion behavior of stainless steel rebars embedded in concrete; and electrochemical impedance spectroscopy study. Electrochim Acta 2014;124:218–24.
[31] González JA, Otero E, Feliu S, Bautista A, Ramírez E, Rodríguez P, et al. Some considerations on the effect of chloride ions on the corrosion of steel reinforcements embedded in concrete structures. Mag Concrete Res 1998;50:189–99.
[32] Page CL. Mechanism of corrosion protection in reinforced concrete marine structures. Nature 1975;258:514–5.
[33] Huet B, L'hostis V, Santarini G, Feron D, Idrissi H. Steel corrosion in concrete: deterministic modeling of cathodic reaction as a function of water saturation degree. Corros Sci 2007;40:1918–32.
[34] Polder RB. Critical chloride content for reinforced concrete and its relationship to concrete resistivity. Mater Corros 2009;60:623–30.
[35] González JA, López W, Rodríguez P. Mecanismos de corrosión en el hormigón armado y factores que controlan su cinética. Rev Metal Madrid 1992;28:297–305.
[36] Fayala I, Dhouibi L, Nóvoa XR, Ben Ouezdou M. Effect of inhibitors on the corrosion of galvanized steel and on mortar properties. Cem Concrete Comp 2013;35:181–9.
[37] Oueslati O, Duchesne J. The effect of SCMs on the corrosion of rebar embedded in mortars subjected to an acetic acid attack. Cem Concrete Res 2012;42:467–75.
[38] Mehta PK, Monteiro PJM. Concrete: microstructure, properties and materials. 2nd ed. Englewood Cliffs, NJ: Prentice Hall; 1993. pp. 32–33.
[39] Bastidas DM, Fernández-Jiménez A, Palomo A, González JA. A study on the passive state stability of steel embedded in activated fly ash mortars. Corros Sci 2008;50:1058–65.
[40] Bautista A, Alvarez SM, Velasco F. Selective corrosion of duplex stainless steel bars in acid. Part 2: effect of the surface strain and numerical analysis. Mater Corros 2015;66:357–65.
[41] Feliu V, González JA, Andrade C, Feliu S. Equivalent circuit for modelling the steel-concrete interface. I. Experimental evidence and theoretical predictions. Corros Sci 1998;40:975–93.
[42] Dhir RK, Jones MR, Ahmed HEH. Determination of total and soluble chlorides in concrete. Cem Concrete Res 1990;20:579–90.
[43] Castro-Borges P, Troconis-de-Rincón O, Moreno EI, Torres-Acosta AA, Martínez-Madrid M. Performance of a 60-years old concrete pier with stainless steel reinforcement. Mater Perform 2002;41:50–5.
[44] Anders KA, Bergsma BP, Hansson CM. Chloride concentration in the pore solution of Portland cement paste and Portland cement concrete. Cem Concrete Res 2014;63:35–7.
[45] Angst U, Elsener B, Larsen CK, Vennesland O. Critical chloride content in reinforced concrete – a review. Cem Concrete Res 2009;39:1122–38.
[46] González JA, Miranda JM, Feliu S. Considerations on reproducibility of potential and corrosion rate measurements in reinforced concrete. Corros Sci 2004;46:2467–85.
[47] Sing H-W, Saraswathy V. Corrosion monitoring of reinforcing concrete structures – a review. Int J Electrochem Sci 2007;2:1–28.
[48] Valek L, Martinez S, Mikulic D, Brnardic I. The inhibition activity of ascorbic acid towards corrosion of steel in alkaline media containing chloride ions. Corros Sci 2008;50:2705–9.
[49] Li L, Dong CF, Xiao K, Yao JZ, Li XG. Effect on pitting corrosion of stainless steel welds in alkaline salt water. Constr Build Mater 2014;68:709–15.
[50] Taylor HFW. Cement chemistry. 2nd ed. London: Thomas Telford; 1997.
[51] Stern M, Geary A. Electrochemical polarization. I. A theoretical analysis of the shape of the polarization curves. J Electrochem Soc 1957;104:56–8.
[52] Andrade C, González JA. Quantitative measurements of corrosion rate of reinforcing steels embedded in concrete using polarization resistance measurements. Werkst Korros 1978;29:515–9.
[53] Poursaee A. Potentiostatic transient technique, a simple approach to estimate the corrosion current density and Stern-Geary constant of reinforcing steel in concrete. Cem Concrete Res 2010;40:1451–8.
[54] Criado M, Bastidas DM, Fajardo S, Fernández-Jiménez A, Bastidas JM. Corrosion behavior of a new low-nickel stainless steel embedded in activated fly ash mortars. Cem Concrete Comp 2011;33:644–52.
[55] Alvarez SM, Bautista A, Velasco F. Influence of strain-induced martensite in the anodic dissolution of austenitic stainless steels in acid medium. Corros Sci 2013;69:130–8.